Geostatistics and Spatial Analysis in Biological Anthropology

John H. Relethford*

Department of Anthropology, State University of New York College at Oneonta, Oneonta, NY 13820

KEY WORDS contour maps; kriging; anthropometrics; Ireland

ABSTRACT A variety of methods have been used to make evolutionary inferences based on the spatial distribution of biological data, including reconstructing population history and detection of the geographic pattern of natural selection. This article provides an examination of geostatistical analysis, a method used widely in geology but which has not often been applied in biological anthropology. Geostatistical analysis begins with the examination of a variogram, a plot showing the relationship between a biological distance measure and the geographic distance between data points and which provides information on the extent and pattern of spatial correlation. The results of variogram analysis are used for interpolating values of unknown data points in order to construct a contour map, a process known as kriging. The methods of geostatistical analysis and discussion of potential problems are applied to a large data set of anthropometric measures for 197 populations in Ireland. The geostatistical analysis reveals two major sources of spatial variation. One pattern, seen for overall body and craniofacial size, shows an east–west cline most likely reflecting the combined effects of past population dispersal and settlement. The second pattern is seen for craniofacial height and shows an isolation by distance pattern reflecting rapid spatial changes in the midlands region of Ireland, perhaps attributable to the genetic impact of the Vikings. The correspondence of these results with other analyses of these data and the additional insights generated from variogram analysis and kriging illustrate the potential utility of geostatistical analysis in biological anthropology. Am J Phys Anthropol 136:1–10, 2008.

An interest in spatial variation underlies much research in biological anthropology. Spatial variation is an important factor to consider when examining population history as well as natural selection and adaptation. Many variables that we study are spatially correlated for one reason or the other, such that geographically proximate populations tend to be biologically similar. This spatial correlation can be due to gene flow among local populations because of the tendency for geographic distance to limit migration. Spatial correlation can also reflect common ancestry, such as would be expected among a group of populations that shared a common set of founders during dispersal into a new area. Depending on the trait/gene, spatial correlation could also result from natural selection acting the same in geographically close and physically similar environments, such as the correlation between skin color and latitude.

There have been a number of approaches used to analyze spatial variation in contemporary, historic, and prehistoric human populations (Barbujani, 2000; Jobling et al., 2004). Graphic representations of a biological distance matrix representing variation among a set of populations, such as cluster analysis and multidimensional scaling, are used to make inferences regarding geographic patterning (e.g., Cavalli-Sforza et al., 1994; Relethford and Crawford, 1995). Other approaches focus on fitting the observed patterns of spatial variation to a model that relates biological and geographic variation, such as the isolation by distance model (e.g., Relethford, 2004). Another approach is spatial autocorrelation analysis, which is particularly useful for identifying and testing hypotheses about complex spatial relationships among populations. Spatial autocorrelation analysis allows detection of patterns of spatial variation among populations, such as clines, isolation by distance, long-distance differentiation, and others, which can in turn be related to evolutionary forces (e.g., Sokal and Oden, 1978a,b; Sokal et al., 1989; North et al., 1999; Barbujani, 2000). Another commonly used approach when analyzing spatial variation, particularly population history, is the use of interpolated contour maps that provide a visual display of spatial variation. Such maps can often be used easily to show gradients and other patterns that can be interpreted in light of population history, such as population dispersions (e.g., Menozzi et al., 1978; Piazza et al., 1981; Cavalli-Sforza et al., 1994). A number of articles have combined different types of geographic analysis, such as spatial autocorrelation and contour maps (e.g., Sokal and Livshits, 1993).

All of these methods (and others) have their advantages and disadvantages, and are best used together to provide the most comprehensive analysis of human biological variation. This article provides background and an example of application of another approach to analyzing spatial variation known as geostatistics. This approach uses a method known as kriging, which pro-

Grant sponsor: National Science Foundation; Grant number: DBS-9120185.

*Correspondence to: Dr. John H. Relethford, Department of Anthropology, SUNY College at Oneonta, Oneonta, NY 13820.
E-mail: relethjh@oneonta.edu

Received 23 July 2007; accepted 4 December 2007

DOI 10.1002/ajpa.20789
Published online 6 February 2008 in Wiley InterScience (www.interscience.wiley.com).

duces interpolated contour maps based on the underlying pattern of spatial correlation. The ultimate goal of geostatistics is a summary graph of the underlying nature of the spatial correlation and a contour map of spatial variation that reflects this correlation. Unlike a combined approach of using spatial autocorrelation analysis and contour maps in tandem (e.g., Sokal and Livshits, 1993), geostatistical analysis is based on a direct link between the pattern of spatial correlation and the interpolation method used to produce a contour map.

Although developed initially for applications in the mining industry, geostatistical analysis can be modified and applied for a variety of problems in biological anthropology. The specific example used here, that of the population history of Ireland, is but one example of many conceivable applications in our discipline. Although other articles have described the underlying method and described its application to epidemiology (Carrat and Valleron, 1992) and human population genetics (Xue et al., 2005), the current article provides a more detailed explanation of the general methodology across the field of biological anthropology. Although a number of recent articles in human genetics have used the kriging method for producing maps of spatial variation (e.g., Malaspina et al., 1998; Torroni et al., 2001; Malhi et al., 2002; Achilli et al., 2004, 2007; Semino et al., 2004; Sengupta et al., 2006; Hill et al., 2007), they do not always provide sufficient detail on underlying patterns of spatial analysis used to produce these maps, or examine potential problems that might have arisen because of violation of the assumptions of the method. As such, this article uses the case study from Ireland to illustrate application of geostatistical analysis in detail.

GEOSTATISTICAL ANALYSIS

To focus the main part of this article on application, the author reviews only the basic elements of geostatistical analysis at this point, deferring many of the technical details to the appropriate place in the data analysis and to the literature, as the focus here is on practical application of the methods. The author starts this discussion with the end product-a contour map that shows visually the geographic distribution of a given variable. There are numerous examples in biological anthropology where the distribution of a given variable is shown on a map, such as the distribution of the sickle cell allele, skin color, cranial shape, and many others. For some purposes, such as mapping common patterns of ancestry and population history, the variable that is mapped is a composite measurement, such as a principal component score of a set of variables (Menozzi et al., 1978). Because we are unlikely to have data for every possible geographic location in a spatial grid, we need to interpolate values between known data points in order to construct a map. Interpolative methods are based on spatial proximity; an unknown data point is more likely to be similar to known data points that are geographically nearby than to known data points farther away in geographic space. One common type of interpolation is inverse distance weighting, where known data points within a given local area are used to predict data values at an unsampled location by weighting the observed data points inversely proportional to their geographic distance from the location. The weighting algorithm can be modified by using different exponents for weighting (inverse distance squared weighting, where the exponent is equal to 2, is a common choice). Although the method is loosely based on the underlying concept of spatial correlation, choice of the weighting exponent is *ad-hoc* and the method tends to readily introduce artifacts of interpolation (Krajewski and Gibbs, 2001). An alternative, central to the field of geostatistics, is to use weighting based on a theoretical distribution inferred from the spatial variability inherent in the data. This estimation method is referred to as kriging, named after mining engineer Danie Krige, whose empirical work led to the development of formal geostatistics theory and method (Clark, 1979).

Geostatistical analysis starts with a variable z which is distributed over geographic space. The ith observation in a data set consists of a value z_i measured at geographic coordinates x_i and y_i (where both x and y are measured on the same scale). The geographic distances between data points and the z values are used to construct an experimental variogram, which is a measure of the dissimilarity in z between data points. The value of the experimental variogram between two data points separated by geographic distance h is a distance measure:

$$\gamma(h) = \frac{(z_i - z_{i+h})^2}{2} \tag{1}$$

The first step in variogram analysis is to compute average values of $\gamma(h)$ and h for different intervals of lag distance and to plot $\gamma(h)$ versus h. The resulting graph provides information on the underlying pattern of spatial correlation, much like the spatial correlograms used in spatial autocorrelation analysis (e.g., Barbujani, 2000). Indeed, variogram distances and measures of spatial autocorrelation are mathematically related (Davis, 2002).

The experimental variogram plot allows analysis of the underlying pattern of spatial correlation, known as the theoretical variogram. For example, a straight horizontal plot suggests an absence of spatial correlation. Other curves showing spatial correlation must be interpreted in terms of processes acting upon the variables of interest. In biological terms, a line with positive slope suggests a spatial cline, and an exponential (or other form of monotonically increasing) curve reaching a plateau suggests isolation by distance. In addition to providing important information on spatial variation, the theoretical variogram is used for interpolation of values for unknown data points on a grid using the kriging method. Kriging is a regression method where data values at unsampled geographic locations are estimated using a weighted average of known data points, where the weighting is based on the theoretical variogram (Davis, 2002). Thus, unlike *ad-hoc* methods of contouring, the weighting method in geostatistical analysis is directly related to the specific underlying pattern of spatial correlation present in a given data set and can often provide the best estimates for unsampled locations (Krajewski and Gibbs, 2001).

Further details of the computational method of kriging can be found in Isaaks and Srivastava (1989) and Davis (2002). Additional information on the underlying statistical theory of geostatistics can be found in Isaaks and Srivastava (1989), Cressie (1993), and Kitandis (1997). Practical issues of data analysis and interpretation are outlined in greater detail in other sources, particularly Clark (1979), U.S. Army Corps of Engineers (1997), Krajewski and Gibbs (2001), and Barnes (2003).

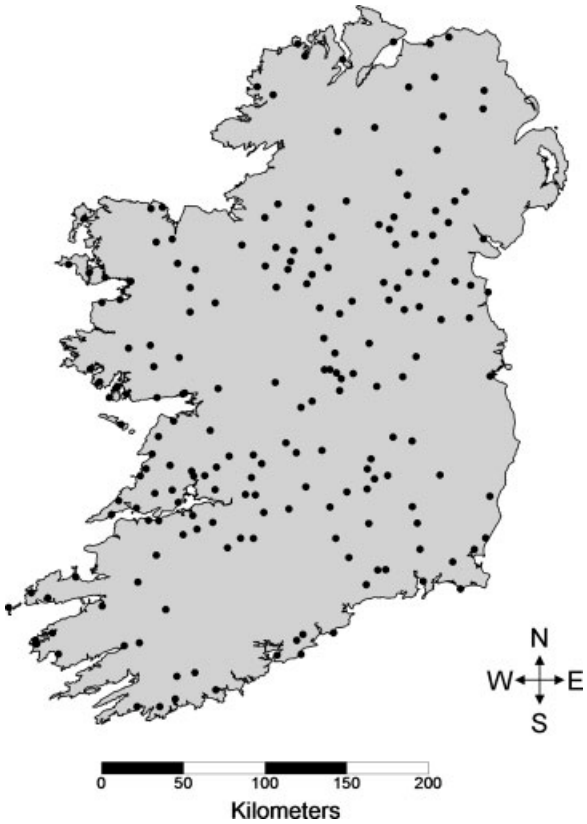

Fig. 1. Location of 197 populations in Ireland used in the analysis. The map was produced using MapViewer, Version 5 (Golden Software) using .e00 files obtained from the Penn State Digital Chart of the World Server (http://www.maproom.psu.edu/dcw/) for the outline map of Ireland and coordinate data for each population from the GEOnet Names Server as described in the text.

MATERIALS AND METHODS

To illustrate the methods of variogram analysis and kriging described thus far, the author apply these methods to a large data set of anthropometric data from Ireland. The data used here consist of anthropometric measurements taken on adult Irish men during the mid-1930s by C. Wesley Dupertuis as part of an anthropological survey of Ireland conducted by Harvard University (Hooton et al., 1955). Dupertuis took anthropometric measurements on almost 9,000 adult males in hundreds of villages, towns, and cities through the island of Ireland (the term "Ireland" used in this article refers to the entire island, which currently consists of two political units-the Republic of Ireland and Northern Ireland). These data were later largely recovered and computerized as described by Relethford and Crawford (1995). Nineteen anthropometric variables are used in the present study. Nine of these variables are body measures: weight, stature, acromial height, dactylion height, span, biacromial breadth, chest breadth, chest depth, and sitting height. The other 10 variables are craniofacial measures: head length, head breadth, head height, minimum frontal breadth, bizygomatic breadth, bigonial breadth, total facial height, upper facial height, nose height, and nose breadth. Another measure, head circumference, was deleted in order to increase sample size substantially (= 578 individuals). The initial data set consisted of 8,384 adult males. Of these, data on age, population of residence, and all 19 measures were available for 7,691 adult males. Cases were then restricted to those individuals who were born in Ireland and had both parents born in Ireland. The final data set was then restricted to populations that had a sample size of 15 or more individuals. These criteria resulted in a final data set of 5,393 adult males in 197 local populations. Sample sizes within populations ranged from 15 to 274 with a mean sample size of 27.4 individuals. The locations of the 197 populations used as the locations in the geostatistical analyses are shown in Figure 1. The spatial coverage in general is comprehensive and there are more than an adequate number of data points. Krajewski and Gibbs (2001) suggest a minimal number of 30 data points for kriging. Two small areas, one along the southern coast and one along the east coast, are more sparsely sampled. In such cases, care must be taken when making any inferences from interpolations in these areas.

Each anthropometric variable was regressed on age and age^2 to remove linear and quadratic age effects and the standardized residuals were then used for further analysis. Population means were then computed for each anthropometric measurement, resulting in a data matrix of 197 populations (rows) and 19 variables (columns). This data matrix was then used for geostatistical analysis. Rather than performing a separate analysis on each of the 19 anthropometric variables, a principal components analysis was performed for the sake of data reduction and to avoid redundancy. This procedure is essentially the same as used by Cavalli-Sforza and colleagues in their construction of synthetic allele frequency maps (Menozzi et al., 1978; Piazza et al., 1981; Cavalli-Sforza et al., 1994). One important difference is that the data matrix of populations by variables used here is complete with no missing data, thus avoiding potential problems with spurious spatial patterns resulting from the interpolation process often used to fill in gaps in a data matrix when constructing synthetic maps (Sokal et al., 1999a; see also Rendine et al., 1999 and Sokal et al., 1999b). The age-adjustment regressions and principal components analysis was performed using SYSTAT, Version 11 (SYSTAT Software).

The component loadings for the four principal components with eigenvalues greater than 1.0 are shown in Table 1. The first principal component is not unexpectedly a size component reflecting body and craniofacial size. The second principal component has moderate to high ($\geq$ 0.4) loadings on head height as well as upper facial height and nose height, reflecting a component that is correlated with total craniofacial height from the chin to the top of the head. The third principal component has moderate loadings on head breadth and bizygomatic breadth reflecting craniofacial breadth. The fourth component shows a contrast between head height and total facial height, reflecting relative craniofacial height.

The longitude and latitude for each population was taken from the GEOnet Names Server (http://earth-info.nga.mil/gns/html/index.html) maintained by the National Geospatial-Intelligence Agency (NGA) for the Republic of Ireland and the United Kingdom (for populations in Northern Ireland). Because a degree of longitude is not equal in length to a degree of latitude, and because variogram construction requires the same scale for spatial coordinates x and y, the geographic coordinates were converted into the Universal Transverse Mercator (UTM) projection. This conversion was made using the Didger computer program, Version 3 (Golden Soft-

TABLE 1. Principal components analysis of town means. Only component loadings whose absolute values are ≥ 0.4 are shown

Variable	Principal component I	II	III	IV
Weight	0.87			
Stature	0.88			
Acromial height	0.82			
Dactylion height	0.76			
Span	0.81			
Biacromial breadth	0.58			
Chest breadth	0.75			
Chest depth	0.53			
Sitting height	0.75			
Head length	0.48			
Head breadth	0.66		0.42	
Head height		0.62		0.49
Minimum frontal breadth	0.57	0.46		
Bizygomatic breadth	0.79		0.45	
Bigonial breadth	0.69			
Total facial height	0.41			−0.58
Upper facial height		0.76		
Nose height	0.47	0.48		
Nose breadth				
Variance explained (%)	41.7	9.6	8.0	6.4

ware) with the World Geodetic System (WGS) 1984 datum (a datum is the name for a standard frame of reference for geographic coordinates and the WGS 1984 datum is a standard for use with the UTM projection). The UTM coordinate system divides the world into 60 zones each representing 6° of longitude. The conversion here used Zone 29N (longitude 12 W to 6 W for the Northern Hemisphere), the zone that includes most of Ireland. The resulting UTM coordinates are in kilometers of easting (relative to the central meridian of the UTM zone) and northing (relative to the equator). Variogram analysis and production of contour maps using the kriging method were performed using the Surfer computer program, Version 8 (Golden Software). Following the program's suggested default, the maximum lag distance used in variogram analysis was one-third the maximum diagonal distance between populations. It is important to use a restricted lag distance when constructing the variogram because $\gamma(h)$ values at large values of h tend to be unreliable and not informative in modeling the shorter range geographic variation typically of interest (Krajewski and Gibbs, 2001). Parameters for variogram models were derived following the step-by-step procedures outlined by Barnes (2003); an initial theoretical variogram was fit to the experimental variogram using the Surfer computer program's interactive interface, and then using the program's "autofit" function to fine-tune the parameter values.

RESULTS

The experimental variogram for the first principal component is shown in Figure 2 (top) using seven spatial lags and is clearly a linear model. Note that the line has a large intercept. Theoretical variograms are characterized by having a value of $\gamma(h) = 0$ when $h = 0$, because by definition the difference between a data point and itself (at $h = 0$) is equal to zero. The discontinuity between the observed data from the experimental variogram and the expectations of the theoretical variogram at $\gamma(0) = 0$ is known as the nugget effect, so named because of the impact on spatial correlation of finding a nugget of gold in a geological deposit. In more general terms, the nugget effect is due to nonspatial variation at a local level, due to both random measurement error as well as variation that occurs on a spatial level at an interval less than the lag distance (Isaaks and Srivastava, 1989; Kitandis, 1997). The result is that two data points that are very close in space might actually have dissimilar values. In terms of biological data, some possible contributors to a nugget effect could be genetic drift, sampling and/or measurement error, or other nonspatial sources of variation. Nugget effects are handled by using a discontinuous function by setting $\gamma(0) = 0$. The experimental variogram in Figure 2 can be described by a theoretical linear variogram with nugget effect of the form

$$\gamma(h) = C_0 + bh \tag{2}$$

where C_0 is the nugget effect and b is the slope of the line, for all values of $h > 0$ (and where $\gamma(h = 0)$ is set equal to 0).

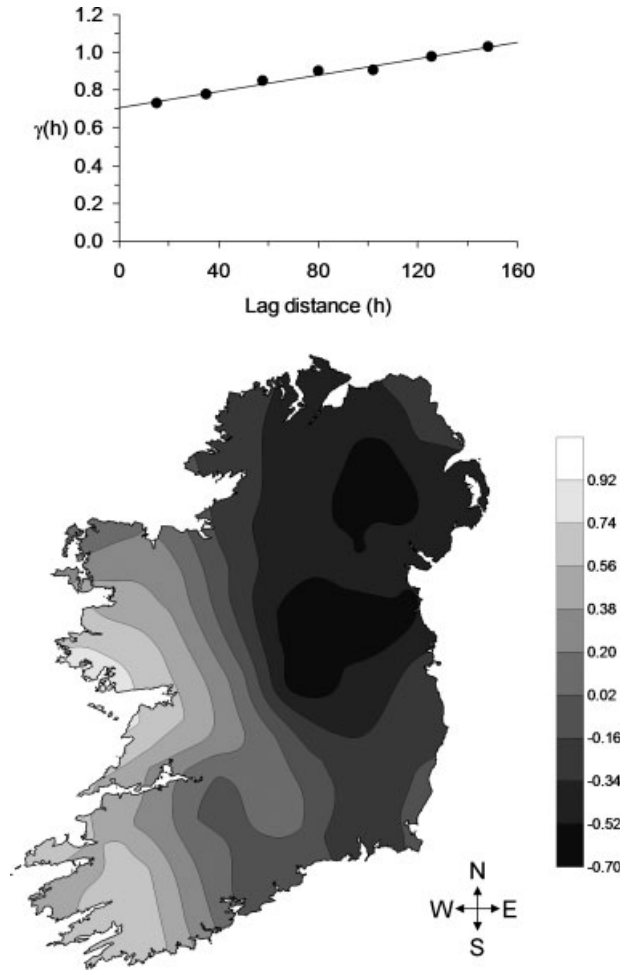

Fig. 2. Geostatistical analysis of principal component I (overall body and craniofacial size) showing the experimental variogram (top) and the contour map produced by kriging (bottom). The experimental variogram is based on seven spatial lags. The data points represent the average value of h and $\gamma(h)$ within each lag interval. The solid line is the theoretical linear variogram [see Eq. (2)] with a nugget effect of $C_0 = 0.7045$ and a slope of $b = 0.0022$. Ten levels are used in the contour map, ranging in value from small (black) to large (light gray) body/craniofacial size.

The linear form of the variogram in Figure 2 shows that the underlying pattern of spatial correlation is a cline, and the large nugget effect shows that a great deal of variation in body/craniofacial size is not spatially correlated. A consequence of a large nugget effect is considerable smoothing of the contour map because the larger the nugget effect, the more equal the weighting of the data points in interpolation. The clinal variation and smoothing is clear looking at the contour map produced by kriging in Figure 2 (bottom). There is a clear east–west cline in body/craniofacial size ranging from smaller values in the east to larger values in the west. A more regular clinal gradient is clearer in the western half of the island, whereas spatial change is less noticeable in the east, suggesting greater homogeneity in body/craniofacial size in eastern Ireland. Examination of the sparsely sampled areas along the southern and eastern coasts (see Fig. 1) does not suggest any major problems with spurious interpolation, as the trends in those areas do not appear unreasonable given the general trends across Ireland. Still, the possibility that the actual variation in those areas could represent local deviations from the general trends cannot be discarded, and no attempt is made here to make inferences regarding variation within those local areas.

Kriging is an exact interpolator, meaning that the estimated value will always be equal to the observed data point at any known location, unlike spatial interpolation methods such as polynomial regression. As such, the residual mean square will be zero. The fit of kriging is instead examined using a cross-validation approach (Isaaks and Srivastava, 1989), where a known data point is excluded and estimated from all remaining data points, and then compared to the observed value. The process is then repeated for each known data point. A useful measure of predictive accuracy is the rank-order correlation between the observed data points and their estimated values under cross-validation (Barnes, 2003). The rank-order correlation from cross-validation for the first principal component in Figure 2 is moderate but not high (= 0.37), showing that the map is good at showing general spatial trends but not that good at replicating local spatial variation. If this were a geological analysis, the results would not suggest high levels of accuracy in predicting where specific mineral deposits would be found, but of course the purpose here is not prediction of spatial variation, but instead a general description of spatial variation, which is abundantly clear from both the variogram and the contour map.

The variogram shown in Figure 2 is an omnidirectional variogram which assumes isotropy such that the value of $\gamma(h)$ depends only on the distance between data points and not on their spatial orientation. This might not always be the case. For example, a cline formed by a population expanding into a region from the southwest and moving to the northeast might create more of a gradient in the southwest–northeast direction than in other directions. Similarly, clines could be formed through natural selection. In either case, when direction as well as distance affects spatial correlation, we have a case of anisotropy, as opposed to the assumption of isotropy used thus far. Anisotropy should be examined in any experimental variogram and isotropy should not be assumed.

Anisotropy is examined by looking to see how the variogram changes as a function of orientation as well as distance. If anisotropy is present, the objective is to define the angles that are orthogonal (90° apart) that produce the maximum and minimum change in $\gamma(h)$ for distance h. In the above example of a southwest–northeast cline, the maximum amount of change would occur along an angle of 45° (degrees are counted in degrees counter-clockwise from the X-axis). Anisotropy is examined by looking at the experimental variogram in different directions by restricting the search for data points within a certain zone of tolerance on both sides of an angle that extends on both sides of a circle. The objective is to find the orthogonal angles that show the greatest ratio of change in $\gamma(h)$. Step-by-step methods on detecting anisotropy are provided by Krajewski and Gibbs (2001) and Barnes (2003). Computationally, adjusting for anisotropy is rather complex (see Isaaks and Srivastava, 1989 and Kitandis, 1997 for details). Essentially, the lag distance h is stretched or compressed along directional axes in order to account for anisotropy.

Here, experimental variograms for the first principal component were examined using the Surfer computer program at different angles and a 30° tolerance and using the program's "autofit" function to fine-tune the initial parameter values found from visual inspection at different possible angles of anisotropy. The best fit was found for anisotropy angles of 100° and 10° (measured counterclockwise from the X axis) and an anisotropy ratio of 4.1. This ratio means that there is 4.1 times more spatial change per unit distance along the 10° angle than at the 100° angle. This is not unexpected given the east–west cline shown in the contour map in Figure 2 which hints at a very slight northeast to southwest direction for the cline (corresponding to the 10° anisotropy angle). The experimental variograms for the 10° and 100° angles are shown in Figure 3, which shows clearly spatial correlation along the 10° (mostly east–west) axis and very little if any spatial correlation along the 100° axis (close to the north–south axis). The contour map produced by kriging using anisotropy is very similar to the isotropic map in Figure 2, although the orientation of the cline is more apparent in that the map in Figure 3 is stretched out a bit more along the 100° axis. Overall, there is not much difference in the general patterns of the map, and the cross-validation rank-order correlation is the same as in the isotropic case (= 0.37).

Another assumption of geostatistical analysis is that there is no trend, such that any pair of points separated by lag distance h should have the same joint probability distribution (Isaaks and Srivastava, 1989). This means that the incremental difference between data points should be the same throughout the study area (Krajewski and Gibbs, 2001). In practical terms, when trend is present the variogram will show $\gamma(h)$ increasing as a parabolic function of lag distance h (U.S. Army Corps of Engineers, 1997; Krajewski and Gibbs, 2001). This results from the fact that any variable with a trend will show a parabolic relationship when plugged into Eq. (1). The presence of trend violates the assumptions of kriging, and is a particular problem if it occurs at smaller values of h. If trend is present, an alternative method of estimation can be used, known as universal kriging (to distinguish it from ordinary kriging, which has been used thus far). Universal kriging consists of fitting a regression model (linear or quadratic) to the data, performing variogram analysis on the residuals, and then adding the trend back into the model. As a point of information, note that "trend" is often referred to as "drift" in the geostatistical literature, but this should not be confused with genetic drift.

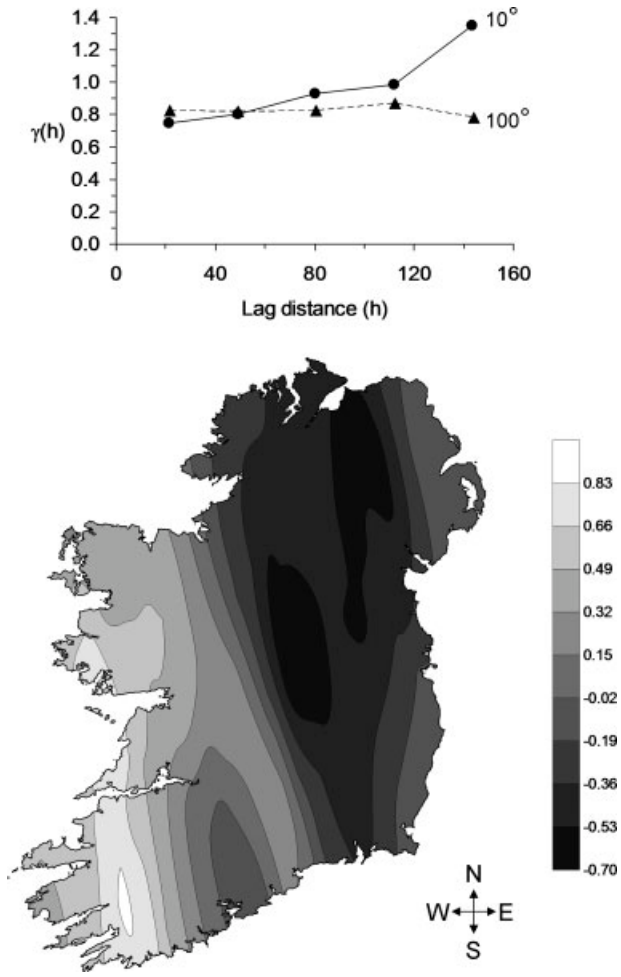

Fig. 3. Anisotropic geostatistical analysis of principal component I (overall body and craniofacial size) showing the experimental variogram (top) and the contour map produced by kriging (bottom). The experimental variogram is shown using five spatial lags at the two orthogonal directions of anisotropy: 100° and 10° and a 30° tolerance. The data points represent the average value of h and $\gamma(h)$ within each lag interval and at each direction ±30°. The solid and dashed lines are used to help distinguish the experimental variograms. The parameters of the theoretical linear variogram (not shown) are a nugget effect of $C_0 = 0.6744$, a slope of $b = 0.0009$, an anisotropy angle of 100°, and an anisotropy ratio of 4.1. Ten levels are used in the contour map, ranging in value from small (black) to large (light gray) body/craniofacial size.

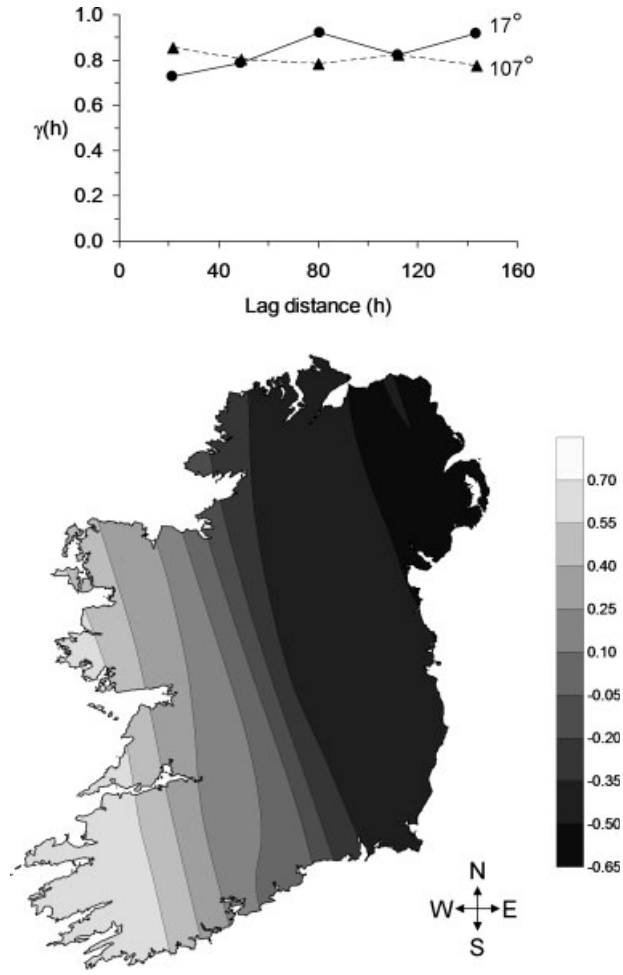

Fig. 4. Universal kriging analysis of principal component I (overall body and craniofacial size) showing the experimental variogram (top) including anisotropy and the contour map produced by universal kriging (bottom). The experimental variogram is shown using five spatial lags at the two orthogonal directions of anisotropy: 107° and 17° and a 30° tolerance. The data points represent the average value of h and $\gamma(h)$ within each lag interval and at each direction ±30° following the subtraction of a linear spatial trend from the data (the trend is then added back to the contour map). The solid and dashed lines are used to help distinguish the two experimental variograms. The parameters of the theoretical linear variogram (not shown) are a nugget effect of $C_0 = 0.7835$, a slope of $b = 0.0001$, an anisotropy angle of 107° and an anisotropy ratio of 5.3. Ten levels are used in the contour map, ranging in value from small (black) to large (light gray) body/craniofacial size.

In Figure 3, the experimental variogram for 10° is slightly parabolic, suggesting a trend that might affect kriging results, and is not unexpected given evidence of a clinal distribution for the first principal component. To examine the impact of the trend on the kriging analysis, the universal kriging method was applied using the Surfer computer program. This was accomplished by fitting a linear trend of the form $z = ax + by + c$ to the data and using the residuals for the variogram analysis. The trend was then added back to the contour map during kriging. Preliminary results showed anisotropy and the results are shown in Figure 4. Overall, the results are very similar to those in Figure 3 with similar anisotropy angles (17° and 107°) and anisotropy ratio (5.3). The nugget effect is higher, reflecting the fact that once a linear trend was removed during universal kriging, there was consequently less spatial correlation apparent in the variogram of the residuals. The contour map is similar to those in Figures 2 and 3, although with more smoothing (as expected given the larger nugget effect). The cross-validation rank-order correlation is slightly lower (= 0.34). Overall, there is not much difference in the three different sets of analyses of the first principal component (Figs. 2–4). All show the east–west cline, clear evidence of anisotropy, and a tendency for somewhat less spatial variation in the eastern half of Ireland. The usual rule of thumb in geostatistical analyses given similar results is to choose the simplest model (Krajewski

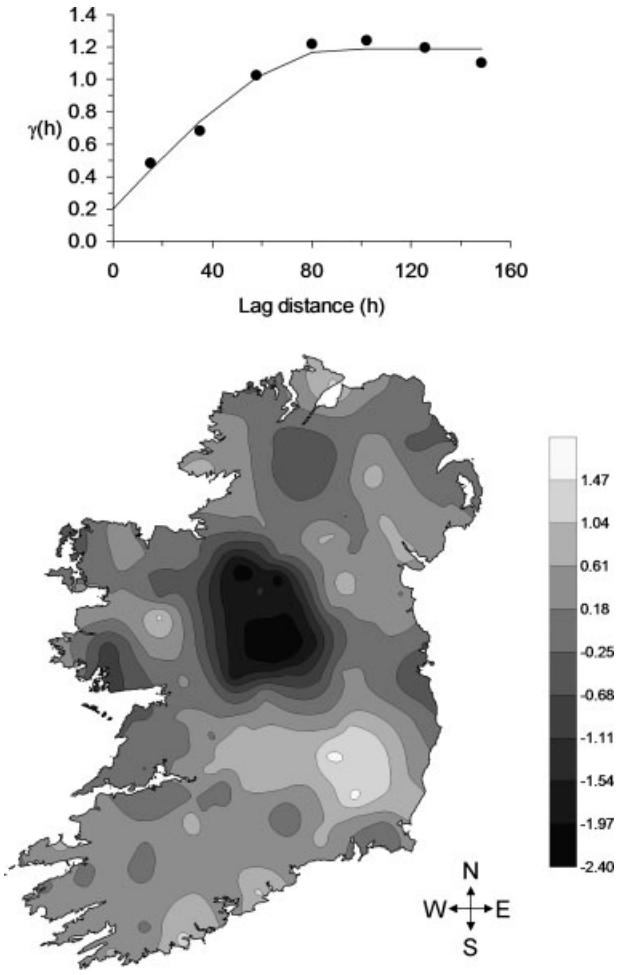

Fig. 5. Geostatistical analysis of principal component II (craniofacial height) showing the experimental variogram (top) and the contour map produced by kriging (bottom). The experimental variogram is based on seven spatial lags. The data points represent the average value of h and $\gamma(h)$ within each lag interval. The solid line is the theoretical spherical variogram [see Eq. (3)] with a nugget effect of $C_0 = 0.1998$, a sill of $C_0 + C = 1.1920$, and a range of $a = 92$ kilometers. Ten levels are used in the contour map, ranging in value from small (black) to large (light gray) craniofacial height.

and Gibbs, 2001). In this case, there would be little point in agonizing over which specific map is best, as they all show the same general trend and all show high nuggets, which means that inferences beyond the most general would be ill-advised. In terms of a general approach to data analysis, the level of detail presented here might not always be necessary, and it might have been sufficient to summarize briefly in the text the results of the anisotropy and universal kriging analyses. The detailed results were provided here, however, to provide the reader with a sense of what the results from such analyses look like. In any event, such analyses should never be skipped.

Figure 5 presents the results of the geostatistical analysis of the second principal component, which represents craniofacial height. The experimental variogram shows what is known as a spherical variogram with a nugget effect, which is an equation of the form:

$$\begin{aligned}\gamma(h) &= C_0 + C\left(\frac{3h}{2a} - \frac{h^3}{2a^3}\right), \quad \text{for } h \le a \\ &= C_0 + C, \quad \text{for } h > a \\ &= 0, \quad \text{for } h = 0\end{aligned} \tag{3}$$

(Cressie, 1997). The spherical model describes an initial linear increase from a nugget effect of C_0, leveling off to a constant value at some point to a maximum value known as a sill. In Eq. (3), the sill is equal to $C_0 + C$, where C is the variation explained by spatial correlation and C_0 is the unexplained variation (nugget effect). The parameter a is known as the range, and refers to the value of h at which $\gamma(h)$ equals the sill. The distance a is the distance at which data points are spatially independent of each other. Thus, the range describes the distance over which there is spatial correlation, with the greatest spatial correlation occurring at small values of h. The variogram in Figure 5 has a small nugget effect, which means that local spatial variation in the second principal component is much better represented than for the first principal component. The cross-validation rank-order correlation is moderate (= 0.41). The spherical variogram shows isolation by distance, with spatial correlation up to the range of $a = 92$ km. Examination of the contour map in Figure 5 shows that the major contribution to the isolation by distance pattern is the rapid changes in craniofacial height that occur in the middle of Ireland, with much less local change occurring elsewhere. Examination of anisotropy (not shown) showed only a mild effect (anisotropy ratio = 1.5 at an angle of 128°) with little impact on the contour map (not shown) or the cross-validation rank order correlation (= 0.40). No evidence of trend was detected. Consequently, the isotropic variogram and contour map shown in Figure 5 were taken as representative of the spatial variation in the second principal component.

Neither the third or forth principal components show much evidence of spatial correlation. As shown in Figure 6 (top), the variogram for the third principal component (craniofacial breadth) is linear, consistent with a cline, but with a very high nugget effect. The contour map (not shown) therefore shows considerable smoothing and indicates a very weak east–west cline essentially paralleling that of the first principal component. Figure 6 (bottom) shows a spherical variogram for the fourth principal component (relative craniofacial height), but with a very high nugget effect. The contour map (not shown) is similar to that of the second principal component, reflecting morphological differentiation in the Irish midlands. Because the results for the third and fourth principal component essentially replicate the patterns shown in the first and second components, but are much weaker in spatial correlation, no further analysis or interpretation is presented.

DISCUSSION

Geostatistical analysis of the Irish anthropometric data shows evidence of two spatial patterns. The first is an overall east–west cline in overall body/craniofacial size with considerable local variation that is not spatially related (i.e., a high nugget effect). Further, this cline shows high anisotropy (little variation in the north–south direction) and less clinal differentiation in the eastern part of the island compared with the west. The second spatial pattern is an isolation by distance effect

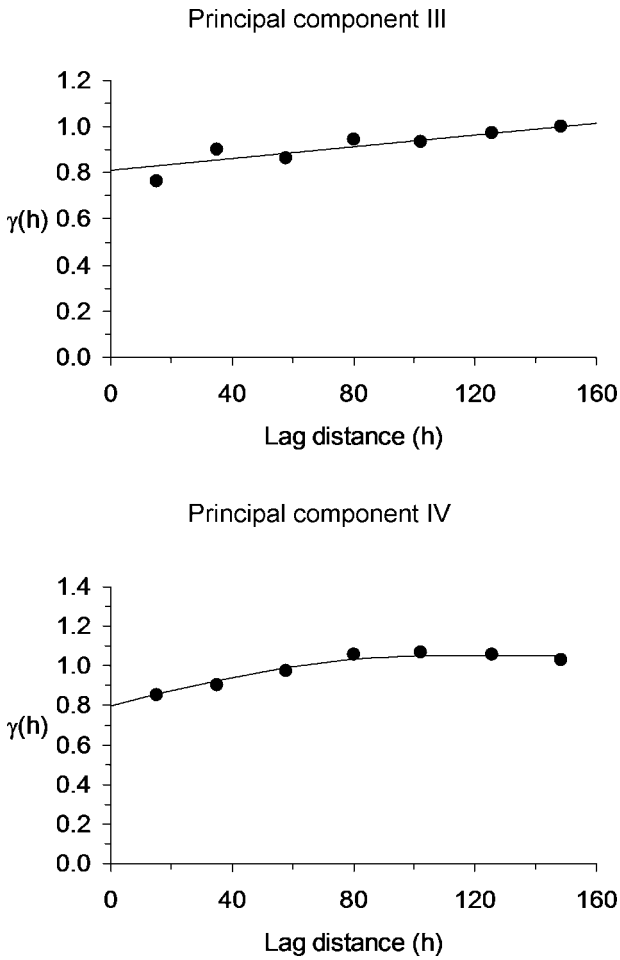

Fig. 6. Variogram analysis for principal components III (top) and IV (bottom). The experimental variograms are based on seven spatial lags. The data points represent the average value of h and $\gamma(h)$ within each lag interval. For principal component III, the solid line is the theoretical linear variogram [see Eq. (2)] with a nugget effect of $C_0 = 0.8121$ and a slope of $b = 0.0013$. For principal component IV, the solid line is the theoretical spherical variogram [see Eq. (3)] with a nugget effect of $C_0 = 0.7982$, a sill of $C_0 + C = 1.0523$, and a range of $a = 102$ kilometers.

seen in craniofacial height where there is rapid change in the Irish midlands. Neither spatial effect showed high cross-validation results, meaning that we would not want to use the contour maps for the purpose of predicting unknown values. Although this lack of predictive accuracy would be a problem in geological applications such as mining, where the researcher would be using the analysis to guide further exploration, it is less of a problem in the present study where the objective is to provide a summary of general patterns of spatial variation. The results shown here are quite useful for detecting general patterns. As with any statistical analysis, interpretation must be kept within reasonable limits.

The usefulness of any type of contour mapping must be viewed in the context of other evidence in order to avoid potential problems in interpretation that result from spurious spatial correlation created from the interpolation process (Sokal et al., 1999a). In this case, the east–west cline is supported by other analyses of Irish population history. Relethford and Crawford (1995) found an east–west effect apparent in their analysis of biological distances among counties. In addition, North et al. (1999) also found evidence of an east–west cline using spatial autocorrelation analysis on a subset of these anthropometric data. Evidence of this cline is not limited to anthropometric variation; an east–west difference has also been detected in studies of blood groups (Hackett et al., 1956; Hackett and Dawson, 1958; Dawson, 1964; Tills et al., 1977), phenylalanine hydroxylase (PAH) haplotypes (O'Donnell et al., 2002), and Y-chromosome markers (Hill et al., 2000). Several explanations have been offered to explain the east–west cline, including continuation of a Neolithic dispersal across Europe into and across Ireland (Hill et al., 2000; O'Donnell, 2002), successive waves of migrants displacing previous inhabitants and pushing them westward (Hooton et al., 1955; North et al., 1999), and the concentration of migrants from England and Wales in the north and east of Ireland over the past 400 years (Tills et al., 1977; Relethford and Crawford, 1995). In the present study, rapid clinal changes are more apparent in the western half of Ireland whereas there is less spatial variation in the east, consistent with the hypothesis of recent historical immigration from England and Wales acting to erase, to some extent, a previous cline created by dispersal. In addition, the areas of smallest body/craniofacial size in the contour map in Figure 2 correspond to the areas receiving immigration during the plantations of James I in the early 17th century (Edwards, 1981). It must be kept in mind, however, that the various hypotheses for an east–west cline are not mutually exclusive and further microgeographic studies using genetic markers are needed to provide further resolution.

A spatial pattern of isolation by distance shows up clearly for the second principal component, where populations in the midlands are distinctly different in terms of having smaller dimensions associated with craniofacial height (head height, upper facial height, and nose height). Previous analysis of biological distances among counties based on anthropometric data showed that the Irish midlands were distinct from other counties (Relethford and Crawford, 1995), a pattern perhaps reflecting the influence of Viking invasion of the midlands. From the 8th through 11th centuries, several Viking invading parties sailed from the Atlantic up the Shannon River to settle at Lough Ree, a lake in the Irish midlands. In addition, comparative biological distance analysis of anthropometrics found that the midlands region is more similar to Norway and Denmark, the ancestral home of Vikings, than are other regions of Ireland (Relethford and Crawford, 1995). Although further analysis (especially DNA-based) will be needed to confirm this hypothesis, the geostatistical analysis here shows the midlands effect even more clearly than the county-based distance analysis performed by Relethford and Crawford (1995). It is particularly interesting that the center of the area of rapid morphological differentiation in the contour map in Figure 5 corresponds with Lough Ree, the center of Viking influence in the midlands.

Although the results of the geostatistical analyses presented here are consistent with other types of analysis of the Irish anthropometric data, a reasonable question would be what information has been added by these analyses. As noted above, the biological distance analyses reported by Relethford and Crawford (1995) did show the basic historical patterns, but not in as much detail. The current analysis shows spatial variation at a much

finer detail because local populations were used rather than counties. The large number of populations used here (n = 197) would make any type of distance map or cluster diagram difficult to interpret as easily as the contour maps reported here. In addition, Figures 2–4 show the difference in clinal variation in the western and eastern regions of Ireland that was not apparent in the county-based analysis. The county-based analysis of Relethford and Crawford (1995) did show the distinctiveness of the Irish midlands but the rapid changes over space apparent in the contour map in Figure 5 were not apparent in the county-based distance analysis. Although North et al.'s (1999) spatial autocorrelation analysis did detect similar spatial trends (clinal and isolation by distance), the actual spatial distribution was not shown, as that requires some sort of contour map. In sum, the historical processes that have operated on Irish anthropometric variation are much clearer from the geostatistical analysis than in previous articles.

Geostatistical analysis provides two important results: (1) variogram analysis gives insight into patterns of spatial correlation, and (2) contour maps produced by kriging provide a visual representation of the data where interpolation is based on the specific underlying pattern of spatial correlation and not on an *ad-hoc* method. Geostatistical analysis offers a number of possibilities in the analysis of biological data, ranging from studies of population history to studies of natural selection. As with any analytic method, there are certain caveats in application that must be kept in mind. First, careful analysis of any problem, be it the reconstruction of population history or the detection of clines produced by natural selection, is best approached using a number of different approaches. Geostatistical analysis should be considered as a supplement to other methods, such as biodistance studies and spatial autocorrelation analysis, and not as a replacement for these methods. Second, geostatistical analysis should not be applied to situations where the data do not meet the requirements of the method, such as an adequate number of data points ($\geq$ 30) (Krajewski and Gibbs, 2001). A third restriction, which applies to the production of any contour map, is to be cautious of situations where spatial interpolation is used to fill in gaps in a data matrix prior to analysis, as this interpolation can create spurious patterns of spatial continuity (Sokal et al., 1999a,b, but also see Rendine et al., 1999). A fourth and critical caveat is that any presentation of the results of a geostatistical analysis must include the entire analysis. A good (nonhuman) example of including variogram analysis and the contour maps produced by kriging is found in Bucci and Vendramin's (2000) analysis of Norway spruce populations. In recent years, a number of studies have presented contour maps produced by kriging based on human molecular genetic data, but have not provided additional details regarding variogram analysis, what type of variogram was used, or analysis of anisotropy or trend (e.g., Malaspina et al., 1998; Torroni et al., 2001; Malhi et al., 2002; Achilli et al., 2004, 2007; Semino et al., 2004; Sengupta et al., 2006; Hill et al., 2007). Complete reporting of geostatistical analysis needs to present the experimental variogram, discussion of the choice of experimental variogram, and consideration of anisotropy and trends if present. Simply presenting the contour map from kriging does not present adequate information for understanding spatial correlation through geostatistical analysis.

ACKNOWLEDGMENTS

The author thanks Michael Crawford for permission to use the Irish anthropometric data used in this article. The author also thanks Ravi Duggarali and Kari North for their assistance in data entry and editing.

LITERATURE CITED

Achilli A, Olivieri A, Pala M, Metspalu E, Fornarino S, Battaglia V, Acceturo M, Kutuev I, Khusnutdinova E, Pennarun E, Cerutti N, Di Gaetano C, Crobu F, Palli D, Matullo G, Santachiara-Benerecetti AS, Cavalli-Sforza LL, Semino O, Villems R, bandelt H-J, Piazza A, Torroni A. 2007. Mitochondrial DNA variation of modern Tuscans supports the Near Eastern origin of Etruscans. Am J Hum Genet 80:759–768.

Achilli A, Rengo C, Magri C, Battaglia V, Olivieri A, Scozzari R, Cruciani F, Zeviani M, Briem E, Carelli V, Moral P, Dugoujon J-M, Roostalu U, Loogväli E-L, Kivisild T, Bandelt H-J, Richards M, Villems R, Santachiara-Benerecetti AS, Semino O, Torroni A. 2004. The molecular dissection of mtDNA haplogroup H confirms that the Franco-Cantabrian glacial refuge was a major source for the European gene pool. Am J Hum Genet 75:910–918.

Barbujani G. 2000. Geographic patterns: how to identify them and why. Hum Biol 72:133–153.

Barnes, R. 2003. Variogram tutorial. Golden, CO: Golden Software. Available online at http://www.goldensoftware.com/variogramTutorial.pdf.

Bucci G, Vendramin GG. 2000. Delineation of genetic zones in the European Norway spruce natural range: preliminary evidence. Mol Ecol 9:923–934.

Carrat F, Valleron A-J. 1992. Epidemiologic mapping using the "kriging" method: application to an influenza-like illness epidemic in France. Am J Epidemiol 135:1293–1300.

Cavalli-Sforza LL, Menozzi P, Piazza A. 1994. The history and geography of human genes. Princeton: Princeton University Press.

Clark I. 1979. Practical geostatistics. London: Applied Science Publishers.

Cressie NAC. 1993. Statistics for spatial data, revised ed. New York: Wiley.

Davis JC. 2002. Statistics and data analysis in geology, 3rd ed. New York: John Wiley & Sons.

Dawson GWP. 1964. The frequencies of the ABO and Rh(D) blood groups from a sample of 1 in 18 of the population. Ann Hum Genet 28:49–59.

Edwards RD. 1981. An atlas of Irish history. London: Methuen.

Hackett WER, Dawson GWP. 1958. The distribution of the ABO and simple Rhesus (D) blood groups in Ireland from a sample of 1 in 37 of the adult population. Irish J Med Sci 387:99–109.

Hackett WER, Dawson GWP, Dawson CJ. 1956. The pattern of the ABO blood group frequencies in Ireland. Heredity 10:69–84.

Hill C, Soares P, Mormina M, Macaulay V, Clarke D, Blumbach PB, Vizuete-Forster M, Forster P, Bulbeck D, Oppenheimer S, Richards M. 2007. A mitochondrial stratigraphy of Island Southeast Asia. Am J Hum Genet 80:29–43.

Hill EW, Jobling MA, Bradley DG. 2000. Y-chromosome variation and Irish origins. Nature 404:351–352.

Hooton EA, Dupertuis CW, Dawson H. 1955. The physical anthropology of Ireland. Papers of the Peabody Museum, Vol. 30, No. 1–2. Cambridge, MA: Peabody Museum.

Isaaks EH, Srivastava RM. 1989. Applied geostatistics. New York: Oxford University Press.

Jobling MA, Hurles ME, Tyler-Smith C. 2004. Human evolutionary genetics: origins, peoples & disease. New York: Garland.

Kitanidis PK. 1997. Introduction to geostatistics: applications in hydrogeology. Cambridge: Cambridge University Press.

Krajewski SA, Gibbs BL. 2001. Understanding contouring: a practical guide to spatial estimation using a computer and basics of using variograms. Boulder: Gibbs Associates.

Malaspina P, Cruciani F, Ciminelli BM, Terrenato L, Santolamazza P, Alonso A, Banyko J, Brdicka R, García O, Gaudiano C, Guanti G, Kidd KK, Lavinha J, Avila M, Mandich P, Moral P, Qamar R, Mehdi SQ, Ragusa A, Stefanescu G, Caraghin M, Tyler-Smith C, Scozzari R, Novelletto A. 1998. Network analyses of Y-chromosomal types in Europe. Northern Africa and Western Asia reveal specific patterns of geographic distribution. Am J Hum Genet 63:847–860.

Malhi RS, Eshleman JA, Greenberg JA, Weiss DA, Schultz Shook BA, Kaestle FA, Lorenz JG, Kemp BM, Johnson JR, Smith DG. 2002. The structure of diversity within New World mitochondrial DNA haplogroups: implications for the prehistory of North America. Am J Hum Genet 70:905–919.

Menozzi P, Piazza A, Cavalli-Sforza LL. 1978. Synthetic maps of human gene frequencies in Europeans. Science 201:786–792.

North KE, Crawford MG, Relethford JH. 1999. Spatial variation of anthropometric traits in Ireland. Hum Biol 71:823–845.

O'Donnell KA, O'Neill C, Tighe O, Bertorelle G, Naughten E, Mayne PD, Croke DT. 2002. The mutation spectrum of hyperphenylalaninaemia in the Republic of Ireland: the population history of the Irish revisited. Eur J Hum Genet 10:530–538.

Piazza A, Menozzi P, Cavalli-Sforza LL. 1981. The making and testing of geographic gene-frequency maps. Biometrics 37: 635–659.

Relethford JH. 2004. Global patterns of isolation by distance based on genetic and morphological data. Hum Biol 76:499–513.

Relethford JH, Crawford MH. 1995. Anthropometric variation and the population history of Ireland. Am J Phys Anthropol 96:25–38.

Rendine S, Piazza A, Menozzi P, Cavalli-Sforza LL. 1999. A problem with synthetic maps: reply to Sokal et al. Hum Biol 71:15–25.

Semino O, Magri C, Benuzzi G, Lin AA, Al-Zahery N, Battaglia V, Maccioni L, Triantaphyllidis C, Shen P, Oefner PJ, Zhivotovsky LA, King R, Torroni A, Cavalli-Sforza LL, Underhill PA, Santachiara-Benerecetti AS. 2004. Origin, diffusion, and differentiation of Y-chromosome haplogroups E and J: inferences on the neolithization of Europe and later migratory events in the Mediterranean area. Am J Hum Genet 74:1023–1034.

Sengupta S, Zhivotovsky LA, King R, Mehdi SQ, Edmonds CA, Chow C-E T, Lin AA, Mitra M, Sil SK, Ramesh A, Usha Rana MV, Thakur CM, Cavalli-Sforza LL, Majumder PP, Underhill PA. 2006. Polarity and temporality of high-resolution Y-chromosome distributions in India identify both indigenous and exogenous expansions and reveal minor genetic influence of Central Asian pastoralists. Am J Hum Genet 78:202–221.

Sokal RR, Jacquez GM, Wooten MC. 1989. Spatial autocorrelation analysis of migration and selection. Genetics 121:845–855.

Sokal RR, Livshits G. 1993. Geographic variation of six dermatoglyphic traits in Eurasia. Am J Phys Anthropol 90:393–407.

Sokal RR, Oden NL. 1978a. Spatial autocorrelation in biology. I. Methodology. Biol J Linn Soc 10:199–228.

Sokal RR, Oden NL. 1978b. Spatial autocorrelation in biology. II. Some biological implications and four applications of evolutionary and ecological interest. Biol J Linn Soc 10:229–249.

Sokal RR, Oden NL, Thomson BA. 1999a. A problem with synthetic maps. Hum Biol 71:1–13.

Sokal RR, Oden NL, Thomson BA. 1999b. Problems with synthetic maps remain: reply to Rendine et al. Hum Biol 71:447–453.

Tills D, Teesdale P, Mourant AE. 1977. Blood groups of the Irish. Ann Hum Biol 4:23–34.

Torroni A, Bandelt H-J, Macaulay V, Richards M, Cruciani F, Rengo C, Martinez-Cabrera V, Villems R, Kivisild T, Metspalu E, Parik J, Tolk H-V, Tambets K, Forster P, Karger B, Francalacci P, Rudan P, Janicijevic B, Rickards O, Savontaus M-L, Huoponen K, Laitinen V, Koivumäki S, Sykes B, Hickey E, Novelletto A, Moral P, Sellitto D, Coppa A, Al-Zaheri N, Santachiara-Benerecetti AS, Semino O, Scozzari R. 2001. A signal, from human mtDNA, of postglacial recolonization in Europe. Am J Hum Genet 69:844–852.

U.S. Army Corps of Engineers. 1997. Practical aspects of applying geostatistics at hazardous, toxic, and radioactive waste sites. Engineer Technical Letter No. 1110–1-175. Washington, DC: Department of the Army.

Xue F-Z, Wang J-Z, Hu P, Li G-R. 2005. The "kriging" model of spatial genetic structure in human population genetics. Acta Genet Sin 32:219–233.